Journal of Organometallic Chemistry xxx (2018) 1–8

Contents lists available at ScienceDirect

Journal of Organometallic Chemistry

journal homepage: www.elsevier.com/locate/jorganchem

Mechanistic insights into asymmetric reductive coupling of isoquinolines by a chiral diboron with DFT calculations

Qinghai Zhou [a, b], Wenjun Tang [c], Lung Wa Chung [a, *]

[a] Department of Chemistry, South University of Science and Technology of China, Shenzhen 518055, China
[b] College of Chemistry, Nankai University, Tianjin 300071, China
[c] State Key Laboratory of Bio-Organic and Natural Products Chemistry, Shanghai Institute of Organic Chemistry, University of Chinese Academy of Sciences, Chinese Academy of Sciences, 345 Ling Ling Road, Shanghai 200032, China

ARTICLE INFO

Article history:
Received 28 November 2017
Received in revised form
30 January 2018
Accepted 1 February 2018
Available online xxx

Keywords:
DFT
Diboron
Isoquinoline
Asymmetric
Reductive coupling
[3,3]-sigmatropic migration

ABSTRACT

We report our complete mechanistic study on the highly diastereo- and enantioselective reductive coupling of isoquinoline templated by a chiral diboron. An uncommon activation mode, activation of the B-B bond *via* double N-B coordination followed by [3,3]-sigmatropic migration was computed to be more preferable over the radical pathway involving the B-B bond homolysis. On the basis of this mechanism, origins of the excellent enantio- and chemoselectivity were found to be driven by less steric repulsion and more secondary orbital interactions in the most favorable reductive coupling transition state. The reductive coupling of dihydroisoquinoline was also investigated and found to have a lower barrier and a larger thermodynamic driving force for the rate-determining second N-B coordination concerted with sigmatropic migration step, compared to isoquinoline. Higher chemoselectivity for the reductive coupling was computed to be achieved by using a strong Lewis-acidic diboron (B_2F_4). These computational results should be helpful for future development of this unusual reductive coupling by diborons.
© 2018 Elsevier B.V. All rights reserved.

1. Introduction

Various activation modes (**eqs. 1**–**4** in Scheme 1) of the B-B bond in diboron compounds [1] have been reported to participate in several important reactions [2] with transition-metal catalysis ([3]; specific examples: Rh [4], Pt [5], Pd [6], Cu [7], Ni [8], Fe [9] and Ir [10]) or with transition-metal-free catalysis ([11,12]). Understanding of the mechanisms of these fascinating and important B-B activation modes (involving transition-metal [6c-e,7,9,10,13] or transition-metal-free [12a-c,12e-f,12h-j,14]) are important and helpful for better development and applications of diboron compounds.

Recently, the metal-free asymmetric reductive coupling of isoquinolines by chiral diborons was reported by Tang and coworkers [15] (Scheme 2). Our preliminary computational mechanistic study suggested that this product was formed through double N-B coordination followed by [3,3]-sigmatropic migration (**eq.5** in Scheme 1). No sign of any radical intermediate was observed by *in-situ* EPR. This uncommon coupling reaction with high stereo- and chemo-selectivity provides convenient and efficient access to bisisoquinolines, which are used as chiral phase transfer agents [16], proton sponge [17], ligand backbones [18] or drugs [19], compared to other earlier synthetic reports [17,18,20]. It is of importance to further explore the detailed reaction mechanism in order to better understand, develop and apply this activation mode.

Compared to earlier reports involving radical intermediates [12f,12g,12i], this B-B activation mode *via* double N-B coordination followed by [3,3]-sigmatropic migration was found to occur in this reductive coupling reaction [15]. This activation mode can be considered as another instance of promoting sigmatropic shifts [21]. Herein, detailed and complete computational mechanistic exploration of this coupling reaction (particularly, the detailed N-B coordination processes, the detailed B-B bond homolysis side reaction as well as, for the first time, energetics evaluated by different methods, the effects of a dihydroisoquinoline substrate and a higher Lewis-acidic diboron (B_2F_4)) is reported.

1.1. Computational details

The reductive coupling of isoquinoline (**IQ**) with a chiral diboron **DB** (Scheme 2, R = H) was chosen as the model reaction. Gaussian

* Corresponding author.
E-mail address: oscarchung@sustc.edu.cn (L.W. Chung).

https://doi.org/10.1016/j.jorganchem.2018.02.001
0022-328X/© 2018 Elsevier B.V. All rights reserved.

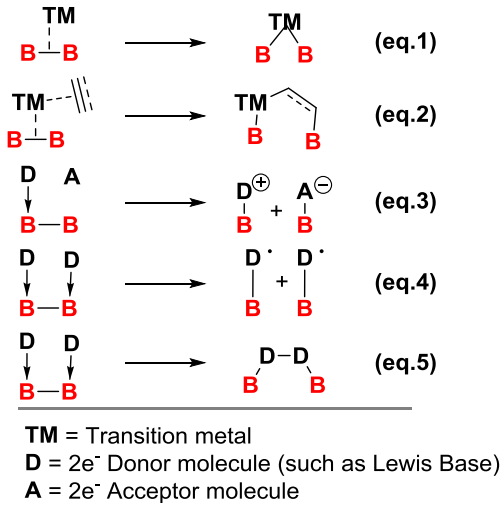

Scheme 1. Various activation modes of the B-B bond in diboron compounds.

09 software package [22] was utilized for all the gas-phase optimization, harmonic vibrational frequency (at 298.15 K) and solvent calculations. The frequency calculations were performed to ensure that one imaginary frequency for all transition states and no imaginary frequencies for all local minima. IRC calculations were also carried out to connect the critical transition states to their corresponding reactant intermediate and product intermediate. (Please refer to SI for our detailed IRC results. 3D structures of all the local minima and transition states along the reaction pathways were also collected in SI.) Solvation effects were included by performing single-point energy calculations with SMD model [23] (solvent = 1,4-dioxane) on the gas-phase optimized geometries at M06/6-31G* level. Unless noted otherwise, this SMD M06/6-31G*//M06/6-31G* methods were used to estimate the corresponding relative free energies in solution (ΔG_{soln}) in this study. For calculations on open-shell transition states and local minima, a broken-symmetry DFT approach was utilized. For the key intermediates and transition states, full optimization in gas phase at B3LYP-D3 [24] and M06-2X [25] levels with 6-31G* were also carried out. Solvation effects were included by performing single-point energy calculations with SMD model (solvent = 1,4-dioxane) on the gas-phase optimized geometries with the corresponding methods. Single-point energy calculations with DLPNO-CCSD(T)/Def2-TZVP method (in which these high-level calculations were carried out by ORCA 4.0.1) [26] in gas phase were also performed. The solvation energy at M06 level were used to estimate DLPNO-CCSD(T) corrected Gibbs free energies in solution. Moreover, gas phase and single-point solvation energy calculations with other functionals

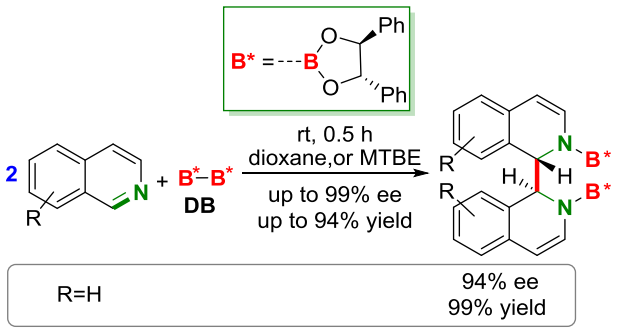

Scheme 2. Experimental observation of reductive coupling of isoquinolines templated by a chiral diboron [15].

(B3LYP-D3, ωB97XD [27], PBE0-D3 [28], and M06-2X) were also performed. For open-shell transition states, NBO 6.0 software [29] was used to perform second-order perturbation theory analysis of Fock matrix in NBO basis. While for closed-shell transition states, NBO 3.1 [30] was used. The 3D models were generated by CYLview [31]. Non-covalent interactions (NCI) analysis was carried out by VMD and Multiwfn [32]. In addition, relative distortion/interaction analysis has also been carried out in which relative distortion energy and relative interaction energy were evaluated based on the two related transition states [33]. The isolated two isoquinoline (**IQ**) or dihydroisoquinoline (**DIQ**) molecules and one diboron molecule were chosen as both energy reference point and reaction starting point.

2. Results and discussion

2.1. Reaction pathways of reductive coupling of *IQ* by *DB*

First, our computational results for the reductive coupling pathways are discussed in this section. As shown in Fig. 1, to form the major product **P**, one N-B coordination should first form to afford **INT1** (ΔG_{soln} = 7.6 kcal/mol), followed by another N-B coordination (*via* **TS1**, 9.4 kcal/mol) to give **INT2** (8.4 kcal/mol), in which the two N-B dative bonds are *syn* to each other. Next, the B-B bond breaking and the C1-C2 bond forming from the two isoquinolines take place *via* **TS2** to generate the major reductive coupling product **P** (−38.2 kcal/mol). This coupling step is thermodynamically favorable and irreversible. Also, the coupling step is suggested to be the rate-determining step (RDS) with the barrier of ~10.8 kcal/mol. The similar steps can take place to afford the enantiomer product $\mathbf{P_{ent}}$ (−35.3 kcal/mol) *via* a rate-determining transition state $\mathbf{TS2_{ent}}$ (12.9 kcal/mol). **TS2** is 2.1 kcal/mol lower than $\mathbf{TS2_{ent}}$, in excellent agreement with the experimental observation (ee = 94% corresponding to $\Delta\Delta G^{\neq}$ = 2.1 kcal/mol, favoring formation of the major product **P** over its enantiomer $\mathbf{P_{ent}}$ in Scheme 2). According to these computational results, the formation of the major product **P** (−38.2 kcal/mol) is both kinetically and thermodynamically more favorable than the enantiomer $\mathbf{P_{ent}}$ (−35.3 kcal/mol).

Along the reaction pathway to the major product **P**, when the N-B coordination proceeds, the B-B bond becomes longer (1.69 Å in **DB**, to 1.72 Å in **INT1**, 1.73 Å in **TS1**, and 1.82 Å in **INT2**, see Fig. 1), and becomes more activated. It is also the case for the reaction pathway to form $\mathbf{P_{ent}}$. The computed B-B and C1-C2 bond distances in **INT2** are 1.82 Å and 2.88 Å, respectively, whereas they become 1.91 Å and 2.77 Å in **TS2**, respectively. These results indicate that **TS2** is a rather early transition state, with small extend of the B-B bond elongation and the C1-C2 bond formation. IRC calculations were performed to confirm that **TS2** connects **INT2** and **P** (see SI for details). The origins of the enantioselectivity will be discussed in section 2.2.

As shown in Fig. 2, the reaction pathway for the formation of the mesomer product $\mathbf{P_{meso}}$ (−38.7 kcal/mol) *via* the [3,3]-sigmatropic migration transition state $\mathbf{TS2_{meso}}$ (16.2 kcal/mol) has a higher barrier by 5.4 kcal/mol, compared to **TS2** (10.8 kcal/mol) leading to the major product **P**. These computational results agree well with the no experimental observation of the mesomer product [15].

2.2. The origins of diastereo- and enantioselectivity

As discussed above, **TS2** (10.8 kcal/mol, $\Delta\Delta G^{\neq}$ = 0.0 kcal/mol) is lower in free energy than $\mathbf{TS2_{ent}}$ (12.9 kcal/mol, $\Delta\Delta G^{\neq}$ = 2.1 kcal/mol) and $\mathbf{TS2_{meso}}$ (16.2 kcal/mol, $\Delta\Delta G^{\neq}$ = 5.4 kcal/mol), which supports good diastereo- and enantioselectivity of the reductive coupling of **IQ** by **DB**. As demonstrated in Table 1, the B3LYP-D3, M06-2X, DPLNO-CCSD(T)//M06, ωB97XD//M06, and PBE0-D3//

Download English Version:

https://daneshyari.com/en/article/7756058

Download Persian Version:

https://daneshyari.com/article/7756058

Daneshyari.com